MODELING FOR SEASONAL MARKED POINT PROCESSES: AN ANALYSIS OF EVOLVING HURRICANE OCCURRENCES[1]

BY SAI XIAO, ATHANASIOS KOTTAS AND BRUNO SANSÓ

University of California, Santa Cruz

Seasonal point processes refer to stochastic models for random events which are only observed in a given season. We develop nonparametric Bayesian methodology to study the dynamic evolution of a seasonal marked point process intensity. We assume the point process is a nonhomogeneous Poisson process and propose a nonparametric mixture of beta densities to model dynamically evolving temporal Poisson process intensities. Dependence structure is built through a dependent Dirichlet process prior for the seasonally-varying mixing distributions. We extend the nonparametric model to incorporate time-varying marks, resulting in flexible inference for both the seasonal point process intensity and for the conditional mark distribution. The motivating application involves the analysis of hurricane landfalls with reported damages along the U.S. Gulf and Atlantic coasts from 1900 to 2010. We focus on studying the evolution of the intensity of the process of hurricane landfall occurrences, and the respective maximum wind speed and associated damages. Our results indicate an increase in the number of hurricane landfall occurrences and a decrease in the median maximum wind speed at the peak of the season. Introducing standardized damage as a mark, such that reported damages are comparable both in time and space, we find that there is no significant rising trend in hurricane damages over time.

1. Introduction. There are many examples of phenomena that occur every year at random times but are limited to a specific season. Two examples of natural events with strong scientific and economic relevance are the following: the Atlantic hurricanes and the Pacific typhoons formed by tropical cyclones that occur between May and November; and the spawning of coho salmon that takes place from November to January. There are some situations where the observational window is limited to a given season, such as wildlife abundance in regions that are not accessible in the winter. In addition, there exist applications where interest lies in studying a physical process during a particular season. One example is the study of extreme precipitation during the dry season in tropical environments. This can be important to guarantee water supplies and also to prevent unexpected disasters. On a different note, studying incidence of online purchase of products during the Christmas season is indispensable for retailers in order to optimize stocking,

advertising, logistics, staffing, and website maintenance and support. In all these examples it is important to understand the underlying mechanism of the seasonal point process. To this end, we need a flexible statistical model that can describe the changes of the process intensity during the season. The model also has to capture the evolution of the intensities from one year to the next, borrowing strength from the whole data set to improve the estimation in a given season. Moreover, the model should be extensible to allow for inference on possible marks associated with the occurrence of the events.

In this paper, we focus on the study of landfalling hurricanes recorded along the U.S. Gulf and Atlantic coasts between 1900 and 2010, and their associated maximum wind speed and damages. Hurricanes are typical seasonal extreme climate events. In light of potential societal and economic impacts of climate change, the obvious question regarding hurricanes is whether there is an intensification of hurricane frequency and an increasing trend of hurricane wind speed and associated damage. A substantial part of the literature on the variability of hurricane occurrences is based on annual counts of events. For example, Elsner, Xu and Jagger (2004) and Robbins et al. (2011) use change point detection methods to find significant increases in storm frequencies around 1960 and 1995. Limiting the analysis to the number of hurricanes per year precludes the description of occurrence variability within each year. Thus, it is not possible to estimate trends in hurricane occurrence during a particular period within the hurricane season, say, a given month. An alternative approach is considered in Parisi and Lund (2000) where the process of hurricane occurrences is modeled with a continuous time-varying intensity function within one year. However, in this case, the inter-annual variability is not accounted for. An approach that models intra-annual as well as inter-annual variability is presented in Solow (1989). The model is applied to a U.S. hurricane data set (different from the one considered here) that consists of monthly counts along the mid-Atlantic coast of the U.S. in 1942–1983. The basic assumption is that the data correspond to a Poisson process with a nonstationary intensity function. This is decomposed into a secular and a seasonal component, estimated from annual and monthly counts, respectively. The analysis indicates no trend during the 1950s and a decreasing trend in the 1970s for the secular component, and a stationary seasonal cycle over time.

The focus on hurricane occurrence is of great importance in a climatological context. However, the frequency of hurricanes provides only a partial measure of the threat that these phenomena represent. When exploring the association of hurricane strength with global warming, Emanuel (2005) calls for research on hurricane potential destructiveness. The disastrous impact to coastal areas draws the attention of the public, and government officials and policy makers need reliable inferences on hurricanes' potential damage for long-term action on economic development and population growth [Pielke and Pielke (1997)]. For instance, in about ten years from Hurricane Fay in 2002 to Hurricane Irene in 2011, hurricane landfalls have

caused around \$235 billion damages in 2013 values, and in 2005 Hurricane Katrina alone caused more than \$80 billion in damage. The devastation raises public concern about societal vulnerability to extreme climate [Katz (2010)].

The statistical literature includes some work on exploring possible trends in landfalling hurricanes' total damages. Katz (2002) uses a compound Poisson process as a stochastic model for total damage. The model consists of two separate components: one for annual hurricane frequency, and a second one for individual hurricane damage. The resulting analysis suggests no upward trend for hurricane damages recorded between 1925–1995, after normalization due to societal changes. Damages are modeled using a log-normal distribution and occurrences are assumed to follow a homogeneous Poisson process, without any time-varying dynamics. Moreover, the literature includes approaches that study the effect of climate and physical factors on hurricane activity [Elsner and Jagger (2013)]. Katz (2002) describes the association between hurricane damages and El Niño. Jagger and Elsner (2006) apply extreme value theory to hurricanes with extreme wind speeds. They assume a homogeneous Poisson process for the occurrences of hurricanes with wind speeds above a threshold, and a generalized Pareto distribution for maximum wind speeds. They find that the quantiles of the distribution of extreme wind speeds vary according to climate factors that affect specific regions differently. Yet another association of hurricane activity with climatic indexes is found in Jagger, Elsner and Burch (2011), where hurricane damages are related to the number of sunspots, as well as to the North Atlantic Oscillation and the Southern Oscillation indexes. Chavas et al. (2012) model the damage index exceedance over a certain threshold using the generalized Pareto distribution with several physical covariates, such as maximum wind speed and continental slope. Murnane and Elsner (2012) use quantile regression to study the relationship between maximum wind speed and normalized economic losses. Essentially, all the papers discussed above focus on estimating trends in hurricane damage and/or its relationship with climate factors. When the point process of hurricane occurrences is modeled, this is done under the simplistic setting of a homogeneous Poisson process.

A fundamental question that remains unanswered by the previously described work is whether the trend of hurricane damage over time is due to the increasing/decreasing frequency or to more/less destructive power of individual hurricanes. These are challenging questions, as natural variability is large and we observe only a handful of hurricanes per season. These issues motivate the presentation of a new statistical method for the analysis of the hurricane data.

In this paper, we propose a flexible joint model for inference on hurricane frequency, maximum wind speed and hurricane damage. Our initial assumption is that the point process of hurricane landfalls follows a nonhomogeneous Poisson process. As such, the process is characterized by nonconstant intensity functions indexed by the hurricane season. Notice that we refer to "intensity" using the point process terminology, and not the climate terminology, where it refers to maximum wind speed. We decompose the intensity functions into normalizing constants, which model annual hurricane frequencies, and density functions, which

model normalized intensities within a season. We use a time series model for the normalizing constants. We then take advantage of the flexibility of Bayesian non-parametric methods to model the sequence of nonhomogeneous density functions. The proposed approach allows for detailed inferences on both the intra-seasonal variations of hurricane occurrences, and the inter-seasonal changes of hurricane frequencies. The latter can be considered on time frames shorter than the whole season, for example, monthly. To our knowledge, this is the first statistical analysis of hurricane behavior that takes such a comprehensive approach. Moreover, to study hurricane damage, we treat maximum wind speed and hurricane damage as marks associated with each hurricane occurrence. We extend the method described above to make inference about marks associated with the time of occurrence of the point process events. As a result, we obtain a full probabilistic description of the dynamics of the process intensities and the distribution of the marks. The application is focused on the hurricane data, but the methodology is suitable in general for time-varying seasonal marked Poisson processes.

The article is organized as follows. Section 2 describes the hurricane data and previous work relevant to this application. We perform an initial analysis of the data, ignoring the year of hurricane occurrence and using a mixture of Beta densities to model the hurricane intensity. This analysis serves to motivate the methodological development, as it clearly suggests that a simple parametric model would not capture the complex shape of the intensity function of occurrences during the hurricane season. Section 3 develops the methodology to incorporate dynamic evolution in the analysis, using dependent Dirichlet process mixture models. We explore the problem of data aggregation and study different aggregation strategies. In Section 4 we present the extension of the model to time-varying marks and apply it to maximum wind speed and hurricane damage. Our results indicate that at the peak of the season, there is an increase in the number of hurricane occurrences, a decrease in the median maximum wind speed and a slight decreasing trend in standardized damage associated with a particular hurricane. Section 5 concludes with a general discussion.

2. Hurricane data. We consider data for 239 hurricane landfalls with reported damages along the U.S. Gulf and Atlantic coasts from 1900 to 2010. The data are available from the ICAT Damage Estimator website (http://www.icatdamageestimator.com). ICAT provides property insurance to businesses and home owners for hurricane and earthquake damage in the United States. The ICAT data are consistent with the landfall summary data of the National Hurricane Center's North Atlantic hurricane database (HURDAT). The scope of the data is restricted to landfalling hurricanes, as we emphasize the analysis of a marked point process where damage is a mark of key interest. Hurricanes are usually defined as tropical cyclones with maximum wind speed of at least 74 miles per hour (mph). With some abuse of terminology, we use "hurricanes" throughout the paper to refer to all the storms in the ICAT data set. This includes 4 tropical depressions,

*Saffir–Simpson hurricane scale. TD: tropical depression; TS: tropical storm; HC 1 to HC 5:
hurricane of category 1 to 5*

Category	TD	TS	HC 1	HC 2	HC 3	HC 4	HC 5
Maximum wind speed (mph)	<39	39–73	74–95	96–110	111–130	131–155	>155

63 tropical storms, 54 hurricanes of category 1, 42 hurricanes of category 2, 59 hurricanes of category 3, 14 hurricanes of category 4, and 3 hurricanes of category 5. The classification follows the Saffir–Simpson hurricane scale in Table 1. The data set includes information on the landing date, base damage, normalized damage to current value, category, maximum wind speed and affected states. A detailed description of the data can be found in Pielke et al. (2008) and the ICAT website. In particular, as discussed in Pielke et al. (2008), there is an undercount of damaging storms prior to 1940. This is an important issue that needs to be considered when quantifying possible trends in the number of hurricane occurrences.

In this application, we consider maximum wind speed and economic damage as marks. Maximum wind speed is defined as the maximum sustained (over one minute) surface wind speed to occur along the U.S. coast. Economic damage is reported as base damage, which is the direct total loss associated with the hurricane's impact in the year when the hurricane occurred. In order to make all storm damages comparable, a standardization method is used to estimate the damages to a baseline year by extending the normalization method from Pielke et al. (2008); see Section 4.2 for details.

The time series of annual hurricane counts is shown in Figure 1. Evidently, hurricane occurrence depicts strong inter-annual variability. Moreover, there are indications of discontinuities, which have been thoroughly considered in the literature. In fact, significant shifts during the middle of the 1940s, 1960s and in 1995 have been identified in Elsner, Xu and Jagger (2004) and Robbins et al. (2011). The changes in the underlying data collection methods, leading to change points in 1935 and 1960, have been explained in Landsea et al. (1999) and Robbins et al. (2011). To explore the variability within the hurricane season, Figure 1 also plots a histogram of hurricane occurrences ignoring the years of the events. The histogram reveals strong intra-seasonal variability, with the peak of the season around September and a concentration of hurricanes around June during the early part of the season. Figure 2 provides further insight on the variability of hurricane occurrence within the season, where we have now applied aggregation by decades. The distribution of hurricane occurrences within one season varies from decade to decade, and the inter-decadal change of hurricane occurrences varies from month to month. This indicates that the hurricane point process intensity during a given season varies over the decades. Here, we assume that such a process corresponds to a nonhomogeneous Poisson process (NHPP).
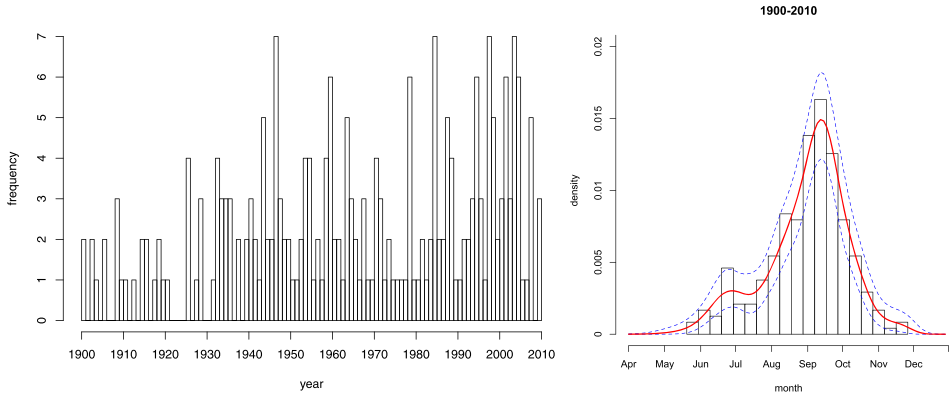
FIG. 1.   *Left panel*: *The time series of annual hurricane occurrences*. *Right panel*: *Histogram* (*with bin width of* 10 *days*) *of hurricane occurrences over months after aggregating all hurricanes into one year*. *The solid and dashed lines denote the point and* 95% *interval estimates of the corresponding NHPP density*, *using the Dirichlet process mixture model discussed in Section* 2.

There is a large body of literature on nonparametric methods to model temporal (or spatial) NHPP intensities and to tackle the analytically intractable NHPP likelihood. Some are based on the log-Gaussian Cox process model [Møller, Syversveen and Waagepetersen (1998), Brix and Diggle (2001), Liang, Carlin and Gelfand (2009)], while others use a Gaussian Cox process model [Adams, Murray and MacKay (2009)]. An approach based on modeling the intensity function using kernel mixtures of weighted gamma process priors is developed in Wolpert and Ickstadt (1998) and Ishwaran and James (2004). The method presented in this paper uses nonparametric mixtures to model a density that, up to a scaling factor, defines the NHPP intensity. The approach was originally developed in Kottas (2006)
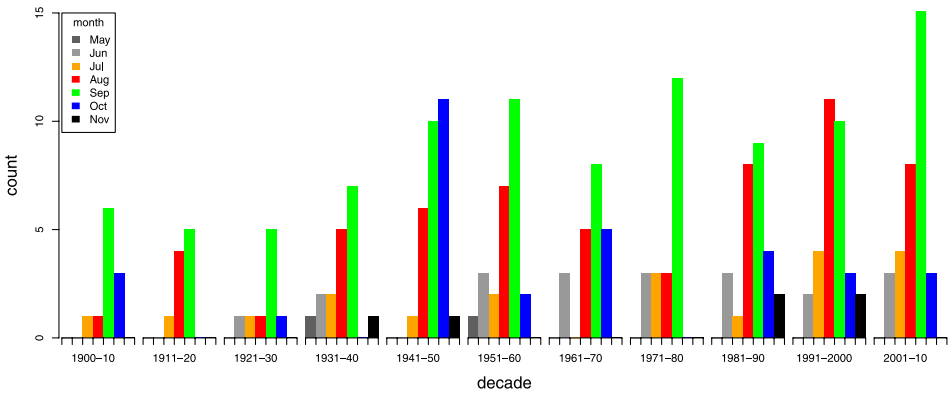

FIG. 2.   *The number of hurricanes within one season aggregated by decades*. *In each decade*, *the number of hurricanes is grouped by months*.

and Kottas and Sansó (2007), with different applications considered by Ihler and Smyth (2007), Ji et al. (2009), Taddy (2010), Kottas et al. (2012) and Kottas, Wang and Rodríguez (2012).

Let $\lambda(t)$ be the NHPP time-varying intensity, with t in a bounded time window $(0, T)$. Inference proceeds by factoring the intensity function as $\lambda(t) = \gamma f(t)$, where $\gamma = \int_0^T \lambda(t) \, dt$ is the total intensity over $(0, T)$; note that $\gamma < \infty$ based on the local integrability of the NHPP intensity function. Hence, the likelihood function induced by the NHPP assumption, using the observed point pattern $\{t_1, \ldots, t_n\}$, is given by $p(\{t_i\}_{i=1}^n | \gamma, f(\cdot)) \propto \exp(-\gamma) \gamma^n \prod_{i=1}^n f(t_i)$, indicating that $f(t)$ and γ can be modeled independently. To develop inference for $\lambda(t)$, we start by rescaling all the observations to the unit interval, thus setting $T = 1$. A convenient choice of distribution that will result in a conjugate prior for γ is the gamma distribution. Alternatively, we can use the reference prior $p(\gamma) \propto \gamma^{-1} 1_{\{\gamma > 0\}}$ [Kottas (2006)]. We model $f(t)$ using the density estimator given by the Dirichlet process (DP) mixture model [Ferguson (1973), Antoniak (1974)]. To complete the model we need to specify a mixing kernel. The kernel of choice in this case is a Beta density, which has the advantages of providing flexible shapes and, being compatible with the compact support of the intensity, avoiding edge effect problems. Using the DP stick-breaking representation [Sethuraman (1994)], the model can be formulated in the following terms:

$$t_i | G, \tau \sim f(t_i | G, \tau) = \int_0^1 \text{Beta}(t_i | \mu\tau, (1-\mu)\tau) \, dG(\mu),$$

$$G(\mu) = \sum_{j=1}^{\infty} w_j \delta_{\mu_j}(\mu),$$

(1)

$$z_j \overset{\text{i.i.d.}}{\sim} \text{Beta}(1, \alpha); \qquad w_1 = z_1,$$

$$w_j = z_j \prod_{r=1}^{j-1} (1 - z_r), \qquad j \geq 2; \qquad \mu_j \overset{\text{i.i.d.}}{\sim} G_0,$$

where G_0 is the DP centering distribution and α is the DP precision parameter. In our case, a convenient choice for G_0 is given by the uniform distribution noting that the Beta mixture kernel is parameterized such that $\mu \in (0, 1)$ is the mean and $\tau > 0$ is a scale parameter.

We apply this model to the hurricane data ignoring the year index. As shown in Figure 1, the estimated density is multi-modal, nonsymmetric and has a non-standard right tail. From this analysis it is clear that a proper description of the hurricane data that assumes an underlying Poisson process requires a nonhomogeneous intensity. Although the initial DP mixture model of Beta densities is flexible enough to capture nonstandard shapes of intensities within a season, it is not capable of describing the evolution of intensities across seasons. To address this problem, we propose in the next section a dynamic extension of the Beta DP mixture model.

3. Modeling time-varying intensities. We seek to model a collection of intensities evolving over years, $\{\lambda_k(t) : k \in \mathcal{K}\}$, where $\mathcal{K} = \{1, 2, \ldots\}$ denotes the discrete-time index set and $\lambda_k(t)$ is the intensity for the season in year k. The model presented in the previous section uses a DP prior to mix over the mean of a Beta kernel. A temporal extension of such a model will have those priors depend on k. To describe the correlation between successive years, the model needs to impose dependence between the priors. As an extension of the DP prior, MacEachern (1999, 2000) proposed to model dependency across several random probability measures. The extension is based on the dependent Dirichlet process (DDP), which provides a natural way to model data varying smoothly across temporal periods or spatial regions. The construction of the DDP is based on the DP stick-breaking definition, where the weights and/or atoms are replaced with appropriate stochastic processes on $\mathcal{K}$. Here, we utilize the "single-p" DDP prior model, where the weights are constant over $\mathcal{K}$, while the atoms are realizations of a stochastic process on $\mathcal{K}$.

3.1. *Nonparametric dynamic model for Poisson process densities.* Denote by $t_{i,k}$, for $i = 1, \ldots, n_k$ and $k = 1, \ldots, K$, the time of the ith event (hurricane landing date) in the kth season, where K is the observed number of seasons and n_k is the observation count in the kth season. Recall that $t_{i,k}$ has been converted to the unit interval. Following the modeling approach discussed in Section 2, the collection of NHPP intensities can be represented by $\{\lambda_k(t) = \gamma_k f_k(t) : k \in \mathcal{K}\}$. To introduce dependence on $\mathcal{K}$, we assume a parametric time series model for $\{\gamma_k : k \in \mathcal{K}\}$ and a DDP mixture model for $\{f_k(t) : k \in \mathcal{K}\}$. The former is described in Section 3.2. The latter is defined as follows:

$$f_k(t) \equiv f(t|G_k, \tau) = \int_0^1 \text{Beta}(t|\mu\tau, (1 - \mu)\tau) \, dG_k(\mu),$$

$$G_k(\mu) = \sum_{j=1}^{\infty} w_j \delta_{\mu_{j,k}}(\mu),$$

where the weights $\{w_j\}$, defined as in (1), are the same across seasons. Thus, the model assumes that observations $t_{i,k}$ in the kth season arise from a mixture of Beta distributions with component-specific means $\mu_{j,k}$ and variances $\mu_{j,k}(1 - \mu_{j,k})/(\tau + 1)$. The distribution for the mean of the Beta mixture kernel is allowed to evolve over $\mathcal{K}$, whereas τ is common to all G_k.

To impose dependence between the collection of random mixing distributions G_k, we replace G_0 in (1) with a stochastic process for the atoms $\{\mu_{j,k} : k \in \mathcal{K}\}$. We thus need a discrete-time process with marginal distributions supported on $(0, 1)$, an appealing choice for which is the positive correlated autoregressive process with Beta marginals (PBAR) developed by McKenzie (1985). For the atom $\mu_{j,k}$, this is defined through latent random variables as follows:

(2) $\mu_{j,k} = v_{j,k} u_{j,k} \mu_{j,k-1} + (1 - v_{j,k}),$

where $\{v_{j,k} : k \in \mathcal{K}\}$ and $\{u_{j,k} : k \in \mathcal{K}\}$ are mutually independent sequences of i.i.d. Beta random variables, specifically, $v_{j,k} \sim \text{Beta}(b, a - \rho)$ and $u_{j,k} \sim \text{Beta}(\rho, a - \rho)$, with $a > 0$, $b > 0$ and $0 < \rho < a$. Using properties for products of independent Beta random variables, it can be shown that (2) defines a stationary process $\{\mu_{j,k} : k \in \mathcal{K}\}$ with $\text{Beta}(a, b)$ marginals. Moreover, the autocorrelation function of the PBAR process is given by $\{\rho b a^{-1}(a + b - \rho)^{-1}\}^m$, $m = 0, 1, \ldots$, and thus ρ controls the correlation structure of the process.

Although the DDP-PBAR prior for $G_{\mathcal{K}} = \{G_k : k \in \mathcal{K}\}$ is centered around a stationary process, it generates nonstationary realizations. In particular, if $\{\theta_k : k \in \mathcal{K}\}$ given $G_{\mathcal{K}}$ arises from $G_{\mathcal{K}}$, then $\text{E}(\theta_k | G_k) = \sum_{j=1}^{\infty} w_j \mu_{j,k}$ and $\text{Cov}(\theta_k, \theta_{k+1} | G_k, G_{k+1}) = (\sum_{j=1}^{\infty} w_j \mu_{j,k} \mu_{j,k+1}) - (\sum_{j=1}^{\infty} w_j \mu_{j,k})(\sum_{j=1}^{\infty} w_j \times \mu_{j,k+1})$.

The Markov chain Monte Carlo (MCMC) method for inference, discussed in Section 3.3 and the Appendix, is based on a truncation approximation to the DDP prior stick-breaking representation. More specifically, $G_k \approx \sum_{j=1}^{N} w_j \delta_{\mu_{j,k}}$, with $w_1, \ldots, w_{N-1}$ defined as in (1), but $w_N = 1 - \sum_{j=1}^{N-1} w_j$. Because the weights are constant across seasons, it is straightforward to choose the truncation level N to any level of accuracy using standard DP properties. For instance, $\text{E}(\sum_{j=1}^{N} w_j | \alpha) = 1 - \{\alpha/(\alpha + 1)\}^N$, which can be averaged over the prior for α to estimate $\text{E}(\sum_{j=1}^{N} w_j)$. Given a tolerance level for the approximation, this expression can be used to obtain the corresponding value N. The truncated version of G_k is used in all ensuing expressions involving model properties and inference results.

3.2. *Time series model for the total intensities.* The Poisson process integrated intensities $\{\gamma_k\}$ can be viewed as a realization from a time series in discrete index space, with positive valued states. We adopt the state–space modeling method with exact marginal likelihood proposed by Gamerman, Rezende dos Santos and Franco (2013). Unlike other time series models that build from a log-Gaussian distributional assumption, this approach provides a conjugate gamma prior, resulting in an efficient MCMC algorithm for posterior simulation. The model is defined by the following evolution equation for γ_k:

$$\gamma_{k+1} = \frac{1}{\omega} \gamma_k \xi_{k+1}, \qquad \xi_{k+1} | \gamma_k, n_{1:k} \sim \text{Beta}(\omega a_k, (1 - \omega) a_k),$$

where ω is a discount factor with $0 < \omega < 1$, ξ_{k+1} is a random multiplicative shock, and $n_{1:k}$ denotes the information available up to time k.

Denote n_0 as the information available initially. Take the initial prior of $\gamma_0 | n_0$ as $\text{Gamma}(a_0, b_0)$. Then, the prior distribution at time k is $\gamma_k | n_{1:k} \sim \text{Gamma}(a_{k|k-1}, b_{k|k-1})$, where $a_{k|k-1} = \omega a_{k-1}$ and $b_{k|k-1} = \omega b_{k-1}$. Based on the NHPP assumption, $n_k | \gamma_k \sim \text{Poisson}(\gamma_k)$, and thus the updated distribution is $\gamma_k | n_{1:k} \sim \text{Gamma}(a_k, b_k)$, where $a_k = \omega a_{k-1} + n_k$ and $b_k = \omega b_{k-1} + 1$. The smoothing updated distribution is

$$(3) \qquad \gamma_k - \omega \gamma_{k+1} | \gamma_{k+1}, n_{1:k} \sim \text{Gamma}((1 - \omega) a_k, b_k).$$

For MCMC posterior inference, we can obtain samples from the full conditionals of the joint vector $\gamma_1, \ldots, \gamma_K$ by first filtering the observations forward to obtain a_k and b_k, $k = 1, \ldots, K$, and then sampling γ_k backward, for $k = K, \ldots, 1$, using the distribution in (3). The discount factor ω is estimated by maximizing the joint log-likelihood function defined by the observed predictive distribution $\log \prod_{k=1}^{K} p(n_k | n_{1:k-1}, \omega)$.

3.3. *Implementation details and posterior inference.* Inference for the scale parameter of the Beta mixture kernel using the fully aggregated data (see Section 2) presented no problems and was quite robust to the choice of the gamma prior assigned to τ. As discussed in more detail in Section 3.4, to estimate evolving hurricane intensities using the DDP mixture model, it is necessary to apply some aggregation of the data into periods of time that comprise more than one year. In this respect, aggregating the data in decades emerges as an appropriate choice. However, the estimation of τ becomes a challenging problem, since in each decade there are still only a handful of hurricanes. In fact, a simulation analysis indicates that reliable estimation of τ requires between 50 to 100 observations per time period. This problem can be explained by the fact that τ partially controls the bandwidth of the Beta kernels, with the width of the kernels in inverse relationship with the size of τ. Thus, when only a few data points are available, τ will tend to be small, allowing wide kernels to use the information from most of the few available data. Such kernels cannot capture the multi-modality of the seasonal hurricane intensity. We thus resort to fixing the value of τ in our analysis of the data aggregated by decade. We assume that the typical width of the Beta kernel corresponds to a month, such that $(1/12)/4$ can be used as a proxy for the corresponding standard deviation $\{\hat{\mu}(1 - \hat{\mu})/(\tau + 1)\}^{1/2}$, yielding $\tau = 575$ when $\hat{\mu} = 0.5$. This is the value of τ used in our analysis. We note that informative priors for τ centered around this value result in similar inferences.

For the centering PBAR process of the DDP prior, we set $a = b = 1$, leading to the default choice of uniform marginal distributions for the $\mu_{j,k}$ covering the entire season between May and November. The DDP prior specification is completed with a uniform hyperprior for the PBAR correlation parameter ρ, and a gamma$(2, 1)$ prior for α. Finally, we set $N = 50$ for the truncation level in the DDP approximation; note that under the gamma$(2, 1)$ prior for α, $E(\sum_{j=1}^{50} w_j) \approx 0.9999578$, using the results discussed in Section 3.1.

We implement the DDP-PBAR model using the blocked Gibbs sampler [Ishwaran and James (2001)] with Metropolis–Hastings steps; see the Appendix for details. Combining the posterior samples for the parameters of the DDP-PBAR model for $\{f_k(t)\}$ and the posterior samples for the parameters of the time series model for $\{\gamma_k\}$, a variety of inferences about hurricane intensity functionals can be obtained.

Of particular interest in our application is the average number of hurricanes within a time interval (t_1, t_2) in the kth season, which is given by

$\Lambda_k(t_1, t_2) = \gamma_k \int_{t_1}^{t_2} f_k(t) \, dt$. We can also obtain the probability of having a certain number x of hurricanes within time interval (t_1, t_2) in the kth season as $\{(\Lambda_k(t_1, t_2))^x / x!\} \exp(-\Lambda_k(t_1, t_2))$. As a consequence, the probability of having at least one hurricane within time interval (t_1, t_2) in the kth season is given by $1 - \exp(-\Lambda_k(t_1, t_2))$. Under the DDP Beta mixture model, $\int_{t_1}^{t_2} f_k(t) \, dt = \sum_{j=1}^{N} w_j \int_{t_1}^{t_2} \text{Beta}(t | \mu_{j,k} \tau, (1 - \mu_{j,k}) \tau) \, dt$.

A further inferential objective is the one-step ahead prediction of the intensity function for the next season, $\gamma_{k+1} \sum_{j=1}^{N} w_j \text{Beta}(t | \tilde{\mu}_{j,k+1} \tau, (1 - \tilde{\mu}_{j,k+1}) \tau)$. Based on the PBAR construction in (2), the conditional distribution for $\tilde{\mu}_{j,k+1}$ given $\mu_{j,k}$ and $v_{j,k+1}$ is a rescaled version of the $\text{Beta}(\rho, 1 - \rho)$ distribution for $u_{j,k+1}$. Hence, for each $j = 1, \ldots, N$, posterior predictive samples for the $\tilde{\mu}_{j,k+1}$ can be readily obtained given draws for the $\mu_{j,k}$ and $v_{j,k+1}$; the former are imputed in the course of the MCMC, the latter can be sampled from their $\text{Beta}(1, 1 - \rho)$ distribution given the MCMC draws for ρ. Therefore, combining with predictive draws for γ_{k+1}, full inference is available for forecasting any functional of the hurricane intensity.

3.4. *Analysis of dynamically evolving hurricane intensities.*

3.4.1. *Data aggregation.* The number of landfalling hurricanes with reported damages during 1900–2010 in the U.S. is 239. On average, there are merely 2 or 3 hurricanes every year, with no hurricane in some years, for example, 1922–1925 and 2009. Thus, the first practical problem we face is that of data scarcity. When modeling the data at the yearly level, the challenge is that it is difficult to analyze a process with so few realizations per year. Hence, we consider aggregating the data over periods of five and ten years, and compare the results under the two different levels of aggregation.

Aggregation over a period of time is based on the assumption that the NHPP densities for all the years corresponding to the aggregated period are the same. For the five year aggregation we have 22 different intensities and for the decadal aggregation we have 11. Data aggregation does not effect the estimation of normalizing constants $\{\gamma_k\}$. In fact, we can apply the model for the $\{\gamma_k\}$ proposed in Section 3.2 to the yearly data, and then aggregate. Figure 3 provides results to compare the two aggregation strategies in the context of forecasting the hurricane intensity and one of its functionals in the next five years 2011–2015. Encouragingly, the results are very similar under the two levels of data aggregation.

Regarding the analysis of historical data, we focus on the month of September. In fact, for the Atlantic hurricane season, August, September and October (ASO) are very important months, as 95% of Saffir–Simpson category 3, 4 and 5 hurricane activity occurs during August to October [Landsea (1993)]. In particular, September is the most frequently occurring month. Figure 4 shows the estimated average number of hurricanes in September under the five year data aggregation. We observe a strong variability, in particular, for the periods 1921–1925, 1966–1970 and
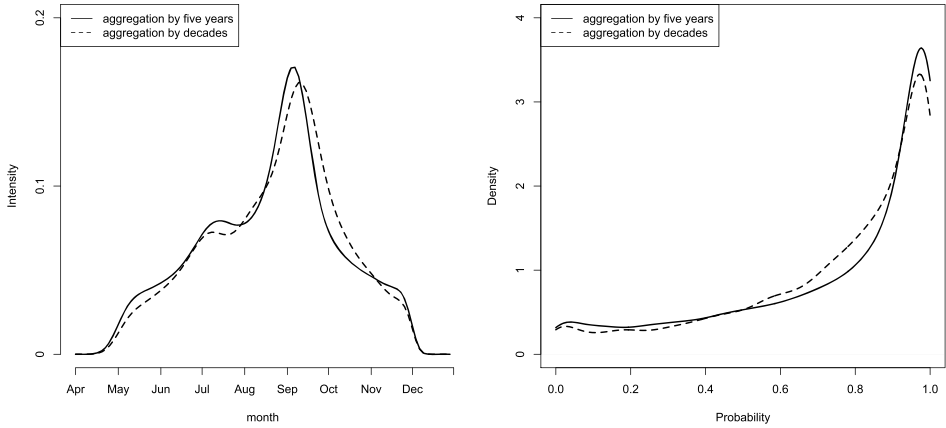
FIG. 3.   *Under the two distinct levels of data aggregation*, *posterior mean estimates for the hurricane intensity in* 2011–2015 (*left panel*) *and posterior densities for the probability of at least one hurricane in May for* 2011–2015 (*right panel*).

1991–1995. This can be attributed to the fact that during 1921–1925 there was no hurricane in September. Moreover, there was only one hurricane in September during 1966–1970, but there were 7 hurricanes in September during both 1961–1965 and 1971–1975. Finally, there was no hurricane in September during 1991–1995, but 10 hurricanes occurred in September during 1996–2000. Thus, even though the prior model is imposing some smoothness, posterior inference results are still strongly affected by the scarcity of observations, even at the level of a five year period. Our resulting inference in the five-year aggregation level reflects the strong variability of hurricane counts in September. More specifically, the clear separa-
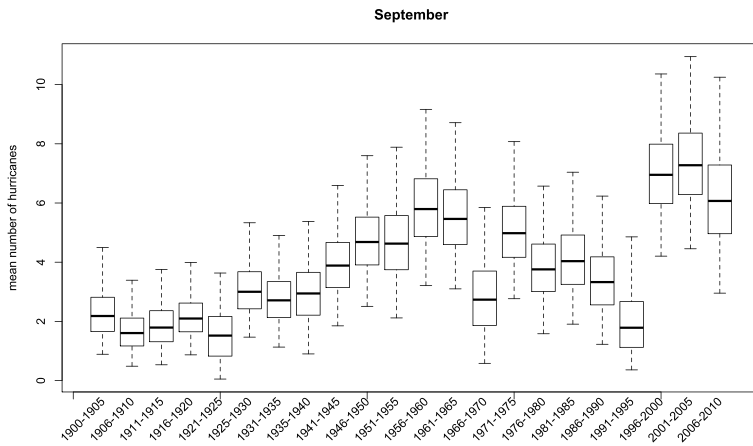

FIG. 4.   *Boxplots of posterior samples for the average number of hurricanes in the month of September across five-year periods from* 1900 *to* 2010.
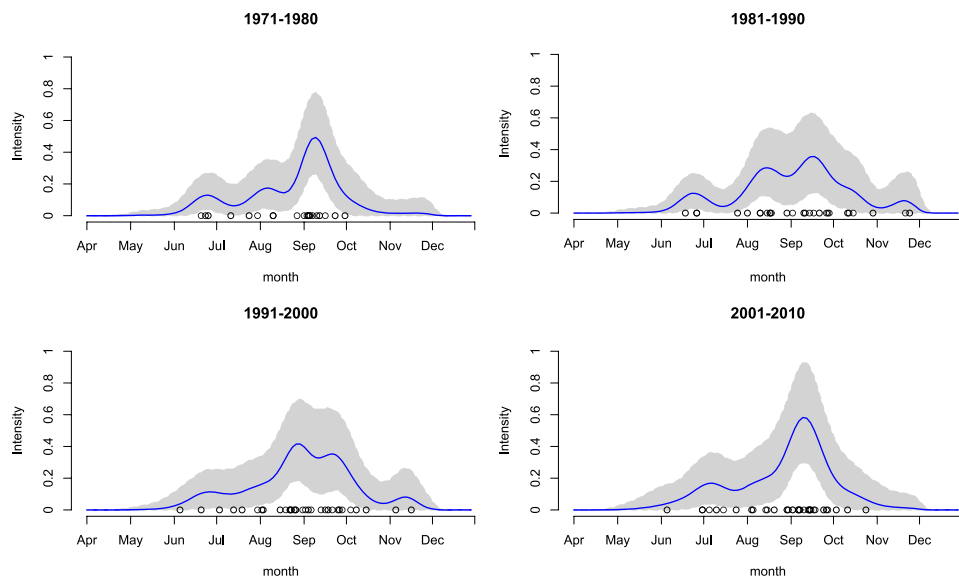
FIG. 5. *Posterior mean estimates (solid line) and 95% intervals (gray bands) of the hurricane intensity during 1971–2010. Points along the horizontal axis correspond to the observations.*

tion of the posterior distributions for the different periods mentioned above gives a probabilistic assessment of significant breakpoints. These are in agreement with the change points detected in Elsner, Xu and Jagger (2004) and Robbins et al. (2011) for the counts over all months. However, in this work we focus on revealing possible long-term trends rather than on anomaly detection. Thus, on the basis of these analyses, for the rest of the paper we focus on data aggregated over decades.

3.4.2. *Evolving hurricane intensities across decades.* Figure 5 presents the estimated intensity functions in the most recent four decades. The estimates fit the data very well, correctly capturing the peaks in ASO and tails in June and November. They show some similarities between the decades, but they adapt to the characteristic of the distribution of hurricane events in each decade. An important product of our probabilistic analysis is the average number of hurricanes in a given time period, which, as discussed in Section 3.3, requires the posterior distribution for both γ_k and G_k. In Figure 6 we present the distributions for the mean number of hurricanes in the peak month of September and the off-season months of May and June, along with the associated observed number of hurricanes. Inference based on our model smooths the data through the decades, especially when a small number of observations are available. Overall, the distribution of the mean number of hurricanes in each decade matches the observations quite well. Both panels depict an increasing trend in the first four decades as well as during the most recent three decades. The former may be an artifact of the under-reporting
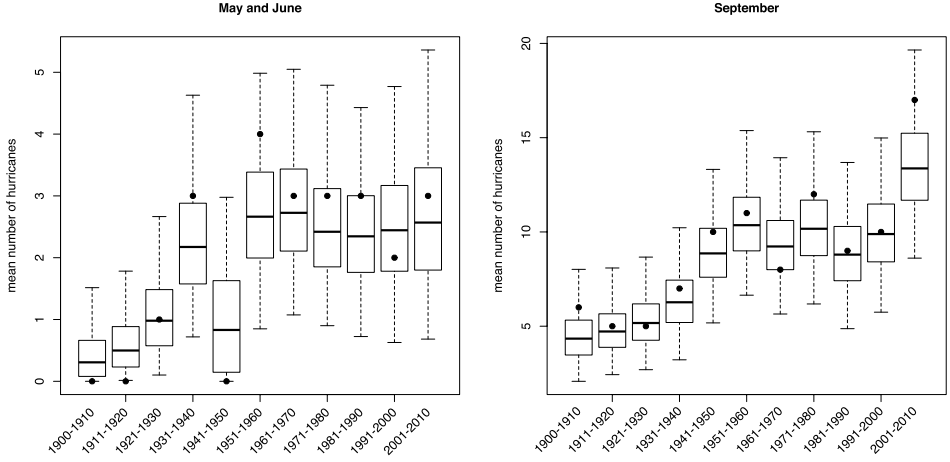
FIG. 6.   *Boxplots of posterior samples of the mean number of hurricanes in early season (May and June) by decade (left panel) and in September by decade (right panel). In both panels, the solid dots indicate the corresponding observed numbers of hurricanes.*

during the beginning of the 20th Century. While the latter is very subtle for the off-season months, it is very strong for the month of September. In fact, the last decade depicts an average number of hurricanes in the peak of the season, which is substantially higher than any other decade on record.

4. DDP model for seasonal marked Poisson processes.   Here, we extend the DDP model, developed in the previous section, to a seasonal marked Poisson process. A marked Poisson process (MPP) refers to a Poisson process with an associated random variable or vector for each event. In our application, $\{t_{i,k} : i = 1, \ldots, n_k\}$ is a point pattern on $(0, T)$ and the marks can be denoted as $\{y_{i,k} : i = 1, \ldots, n_k\}$ on mark space Y. Thus, the realization from the marked point process in the kth decade is $\{(t_{i,k}, y_{i,k}) : t_{i,k} \in (0, T), y_{i,k} \in Y\}$. A MPP can be defined as a Poisson process on the joint marks-points space with intensity function φ on $(0, T) \times Y$. In particular, the marking theorem [Møller and Waagepetersen (2004)] states that a MPP is a NHPP with intensity function given by $\varphi(t, y) = \lambda(t) f(y|t)$, where $\lambda(t)$ is the marginal temporal intensity function, and the conditional mark density $f(y|t)$ depends only on the current time point t.

4.1. *The DDP-AR model.*   We extend the methodology from Taddy and Kottas (2012) for MPPs based on joint mixture modeling on the marks-points space. This modeling approach yields flexible inference for both the marginal temporal intensity and for the conditional mark distribution. Here, it is utilized to develop a model for the collection of hurricane MPPs evolving over decades. We will refer to the full model as the DDP-AR model, since, in addition to the PBAR structure, it

incorporates autoregressive processes to model the conditional evolution of marks over time.

The marks are given by the maximum wind speed for each hurricane and the associated economic damages. Instead of using the total dollar amount of hurricane damage, we define a standardized damage, which is calculated as a proportion of total wealth with respect to a reference region and a baseline year (see Section 4.2). The resulting NHPP is defined in a three-dimensional space comprising time, maximum wind speed and standardized damage. Maximum wind speed and standardized damage are transformed by taking logarithms and subtracting the global average of the log-transformed values. We denote $y_{i,k}$ and $z_{i,k}$ as, respectively, the transformed maximum wind speed and the transformed standardized damage of the ith hurricane in the kth decade. For the three-dimensional intensity function, $\varphi_k(t, y, z)$, we use the factorization $\gamma_k f_k(t, y, z)$, where $\{\gamma_k\}$ follows the time series model presented in Section 3.2. Regarding the density function, we use a DDP mixture with a product of univariate kernel densities for time and marks. Thus, the dependence among time and marks is introduced by the mixing distribution. We retain the Beta kernel density for time and use Gaussian kernel densities on the log scale for the two marks, mixing on the mean of each kernel component. Hence, the DDP mixture model for $f_k(t, y, z)$ can be expressed as

$$(4) \qquad \int \mathrm{Beta}\big(t|\mu\tau, (1 - \mu)\tau\big)\mathrm{N}\big(y|\nu, \sigma^2\big)\mathrm{N}\big(z|\eta, \zeta^2\big)\, dG_k(\mu, \nu, \eta),$$

where $G_k(\mu, \nu, \eta) = \sum_{j=1}^{N} w_j \delta_{(\mu_{j,k}, \nu_{j,k}, \eta_{j,k})}(\mu, \nu, \eta)$. The locations ν and η of the normal kernels are allowed to change across decades. The scales σ^2 and ζ^2 are the same across decades, serving as adjusting parameters for the bandwidth of the kernels. Conditionally conjugate inverse gamma priors are assumed for σ^2 and ζ^2.

Dependence across decades for maximum wind speeds and standardized damages is obtained through AR(1) processes for the respective kernel means $\{\nu_{j,k} : k \in \mathcal{K}\}$ and $\{\eta_{j,k} : k \in \mathcal{K}\}$:

$$\nu_{j,k}|\nu_{j,k-1} \sim \mathrm{N}\big(\beta\nu_{j,k-1}, \sigma_1^2\big), \qquad \eta_{j,k}|\eta_{j,k-1} \sim \mathrm{N}\big(\phi\eta_{j,k-1}, \sigma_2^2\big)$$

with inverse gamma priors assigned to σ_1^2 and σ_2^2, and uniform priors on $(-1, 1)$ placed on β and ϕ. Since the DDP prior structure for $G_{\mathcal{K}} = \{G_k : k \in \mathcal{K}\}$ in (4) extends the one for the DDP-PBAR model, we retain the result about nonstationary realizations given $G_{\mathcal{K}}$, extending the argument in Section 3.1. When the random measures G_k are integrated out, we obtain $\mathrm{E}(y_k) = 0$, $\mathrm{Var}(y_k) = \mathrm{E}(\sigma^2) + (1 - \beta^2)^{-1}\mathrm{E}(\sigma_1^2)$ and $\mathrm{Cov}(y_k, y_{k+1}) = \beta(1 - \beta^2)^{-1}\mathrm{E}(\sigma_1^2)$, with analogous results for the z_k. These expressions can be of help for prior specification.

The MCMC method for the DDP-AR model involves an extension of the posterior simulation algorithm described in the Appendix.[2] As the marks are associated with normal AR(1) processes and conditionally conjugate priors are used,

---

[2]The code to implement the DDP-AR model (as well as the DDP-PBAR model) is available from the first author's website at http://users.soe.ucsc.edu/~sxiao/research.html#software.

all the parameters associated with marks have closed-form full conditionals. Finally, since the normalizing factors (required for the standardization of damages) corresponding to the period 2005–2010 are not available, the MCMC algorithm includes steps to impute the missing standardized damages for those years.

4.2. *Standardization of hurricane damages.* The purpose of standardizing hurricane damages is to isolate societal and spatial factors that affect the amount of damage and are not considered in the model. There exist several methods to adjust the economic damages of past hurricanes to today's value [Pielke et al. (2008), Schmidt, Kemfert and Hoeppe (2010), Collins and Lowe (2001)]. Here, we define standardized damage as an extension to the method in Pielke et al. (2008).

The hurricane data set includes base damage and normalized damage. Base damage is calculated as the total landfall year dollar value of the damage caused by a hurricane. Such amount is converted to the dollar value corresponding to the latest year in the record by normalizing for inflation, wealth and population over time. Denote inflation, wealth per capita and affected county population in year t as I_t, W_t and P_t, respectively. Equation (5) shows the normalization of the damage due to a hurricane landing in year t to values in year s:

$$(5) \qquad \text{normalized.damage}_s = \text{base.damage}_t \times \frac{I_s}{I_t} \times \frac{W_s}{W_t} \times \frac{P_s}{P_t}.$$

This normalization method yields the estimated damages of all hurricanes in today's value but in the same region, for example, the damages caused by Katrina 2005 if it occurred under societal conditions in Louisiana affected counties in 2013.

To make hurricane damages comparable, we have to adjust for inflation and account for the fact that much more damage will be caused if the hurricane lands in densely populated and wealthier counties than in scarcely populated and poor regions. Thus, we have to remove both a spatial and societal factor from the damage, so that the model can explore the pure association between damages and climate variability. Hence, we define standardized damage as

$$\text{standardized.damage} = \frac{\text{base.damage}_t}{I_t \cdot W_t \cdot P_t}.$$

Such a quantity can be interpreted as a base damage normalized to a reference year's value in a reference region; in the reference year and region, the inflation factor, wealth per capita and population are all equal to 1. This method removes the difference in hurricane damages due to the landing years and locations. Neumayer and Barthel (2011) and Chavas et al. (2012) developed similar ideas normaliz-
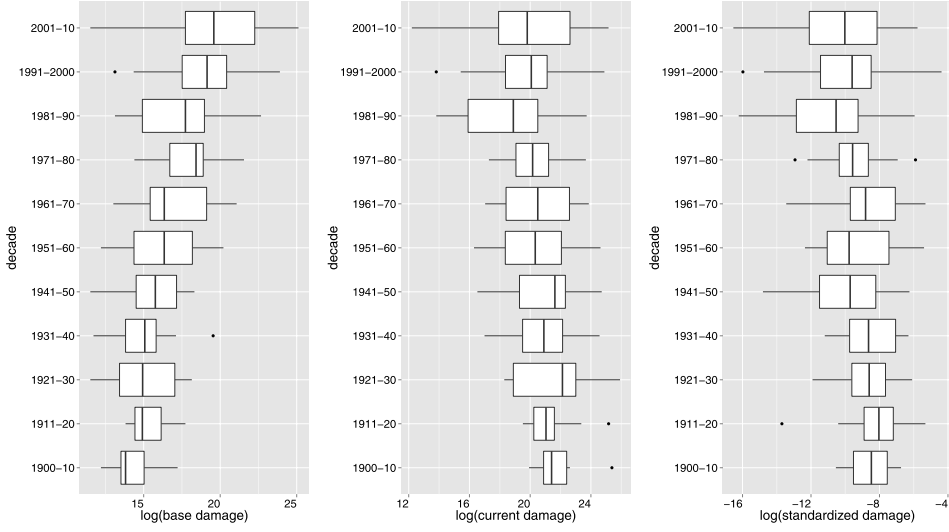
FIG. 7. *Data box plots across decades for log-transformed base damages* (*left panel*), *damages normalized to current values* (*middle panel*) *and standardized damages* (*right panel*).

ing damages by using base.damage$_t$/wealth$_t$, where wealth$_t$ is the total wealth of the affected regions. They interpret the standardized damage as a relative damage, termed actual-to-potential-loss ratio. Note that the denominator we use, $I_t \cdot W_t \cdot P_t$, is an approximation of wealth$_t$. All inferences presented in Section 4.4 that involve hurricane damage refer to standardized damage. Note that, if the normalizing factors are provided, actual hurricane damages for a given affected region and year can be obtained from standardized damages. It is important to notice that the normalizing factors prior to 1925 have larger uncertainties compared to those for later periods [Pielke et al. (2008)]. This problem is compounded with the already mentioned issue of underreporting of hurricanes in the early part of the 20th Century. The reader should keep this in mind when interpreting the results in the following sections.

To visualize the effect of the conversion on damage values, Figure 7 shows three different calculations for hurricane damage and their change over decades. The base damage depicts an increasing trend over decades, which disappears after normalization and standardization.

4.3. *Inference.*   For a marked point process the typical inference of interest is for the distribution of the marks, conditional on time. To obtain inference about different functionals of the conditional mark distribution, we use the available posterior samples of the joint density $f_k(t, y, z)$. Specifically, conditional inference for

maximum wind speed is obtained from

$$f_k(y|t, G_k) = \frac{f_k(y, t|G_k)}{f_k(t|G_k)}$$

(6)
$$= \frac{\sum_{j=1}^{N} w_j \, \text{Beta}(t|\mu_{j,k}\tau, (1 - \mu_{j,k})\tau) \text{N}(y|\nu_{j,k}, \sigma^2)}{\sum_{j=1}^{N} w_j \, \text{Beta}(t|\mu_{j,k}\tau, (1 - \mu_{j,k})\tau)}$$

$$= \sum_{j=1}^{N} w_{j,k}^*(t) \text{N}(y|\nu_{j,k}, \sigma^2),$$

where $w_{j,k}^*(t) = \frac{w_j \, \text{Beta}(t|\mu_{j,k}\tau, (1-\mu_{j,k})\tau)}{\sum_{j=1}^{N} w_j \, \text{Beta}(t|\mu_{j,k}\tau, (1-\mu_{j,k})\tau)}$. Of particular importance is the distribution of maximum wind speed conditional on a specific time period, for example, the peak season ASO or a particular month. Suppose that the time period of interest corresponds to the interval (t_1, t_2). The density conditional on (t_1, t_2) can be developed as

$$f_k(y_0|t \in (t_1, t_2), G_k)$$

(7)
$$= \frac{\lim_{\Delta y_0 \to 0}(1/\Delta y_0) \Pr(y \in (y_0, y_0 + \Delta y_0], t \in (t_1, t_2)|G_k)}{\Pr(t \in (t_1, t_2)|G_k)}$$

$$= \sum_{j=1}^{N} h_{j,k}^* \text{N}(y_0|\nu_{j,k}, \sigma^2),$$

where $h_{j,k}^* \equiv h_{j,k}^*(t_1, t_2) = \frac{w_j \int_{t_1}^{t_2} \text{Beta}(t|\mu_{j,k}\tau, (1-\mu_{j,k})\tau)\mathrm{d}t}{\sum_{j=1}^{N} w_j \int_{t_1}^{t_2} \text{Beta}(t|\mu_{j,k}\tau, (1-\mu_{j,k})\tau)\mathrm{d}t}$.

In equations (6) and (7), both the weights, $w_{j,k}^*(t)$, $h_{j,k}^*$, and the mixing components, $\nu_{j,k}$, change with the decade index k; importantly, the former are time dependent, thus allowing local learning under the implied location normal mixtures. Hence, the model has the flexibility to capture general shapes for the conditional mark distribution which are allowed to change across decades in a nonstandard fashion. Analogous expressions hold for the conditional distribution of standardized damage. Moreover, since equation (4) provides the joint density of time, maximum wind speed and standardized damage, we can obtain inference for a mark conditional on an interval of the other mark and an interval of time. For instance, we can explore the distribution of damage conditional on the hurricane category as defined by different intervals of maximum wind speed; see Table 1.

The time evolution of hurricane occurrences and the marks are controlled by autoregressive processes. One-step ahead prediction of joint time-mark distributions can be obtained by extending the method described in Section 3.3 with additional sampling for the $\{\nu_{j,k+1}\}$ and $\{\eta_{j,k+1}\}$ from the AR(1) processes that form the building blocks of the DDP prior.

4.4. *Results*. We applied the DDP-AR model to the full data set involving hurricane occurrences across decades and the associated maximum wind speeds and standardized damages. The hyperpriors for the time component of the DDP mixture model were similar to the ones discussed in Section 3.3 for the DDP-PBAR model; τ was again fixed. For the variances of the Gaussian mixture kernels and the variances of the corresponding AR(1) processes for the DDP prior, we used $\sigma^2 \sim \text{IG}(3, 2)$, $\zeta^2 \sim \text{IG}(3, 10)$ and $\sigma_1^2 \sim \text{IG}(3, 2)$, $\sigma_2^2 \sim \text{IG}(3, 10)$. Here, the shape parameter of each inverse gamma prior is set to 3, which is the smallest (integer) value that ensures finite prior variance. The prior means were specified using the expressions for the marginal variances of maximum wind speed and standardized damage (see Section 4.1) with β and ϕ replaced by their prior mean at 0. In particular, we set $\text{E}(\sigma^2) = \text{E}(\sigma_1^2) = 0.5(R_y/4)^2$ and $\text{E}(\zeta^2) = \text{E}(\sigma_2^2) = 0.5(R_z/4)^2$, where R_y and R_z denotes the range of the $y_{i,k}$ and $z_{i,k}$, respectively.

The posterior distribution for the number of distinct mixing components is supported by values that range from 10 to 16. The 95% posterior credible interval for ρ is given by $(0.73, 0.87)$, resulting in a $(0.59, 0.79)$ 95% credible interval for the PBAR correlation. On the other hand, the 95% posterior credible intervals for β and ϕ are, respectively, $(-0.14, 0.79)$ and $(-0.24, 0.81)$, indicating more variability in the estimated correlation of the AR(1) centering processes for the DDP prior. Retaining the uniform priors for ρ, β and ϕ, we performed a prior sensitivity analysis for the variance hyperparameters. The parameters σ^2 and σ_1^2 associated with maximum wind speed are relatively sensitive to the prior choice, while the parameters ζ^2 and σ_2^2 for standardized damage are quite stable. Overall, posterior inference results are robust to moderate changes in the prior hyperparameters.

For inference, we focus on the densities of maximum wind speed and logarithmic standardized damage conditional on events occurring in the early season and the peak season. Figure 8 shows the comparison between the maximum wind speed densities conditional on June and September in each decade. We observe that maximum wind speeds in September are higher than in June for all decades. In the 1960s the density has a very long left-hand tail, even showing evidence of two modes. Noteworthy in the last four decades is the increasing accumulation of density on lower values of maximum wind speed. The fact that maximum wind speeds in September are decreasing is confirmed by the plot in the lower panel of Figure 8, where both point and interval estimates support a decreasing trend for the median maximum wind speed in September. In particular, after peaking at more than 110 mph in the 1920s, the posterior point estimate has settled at around 85 mph in the last decade.

Figure 9 (top left panel) shows the density of standardized damages (on the log scale) conditional on the early season and the peak season. The densities of standardized damages in MJJ (May–June–July) are quite similar throughout all decades, while the densities in ASO show a moderate decreasing trend across decades. Figure 9 (bottom left panel) plots point and interval estimates for the
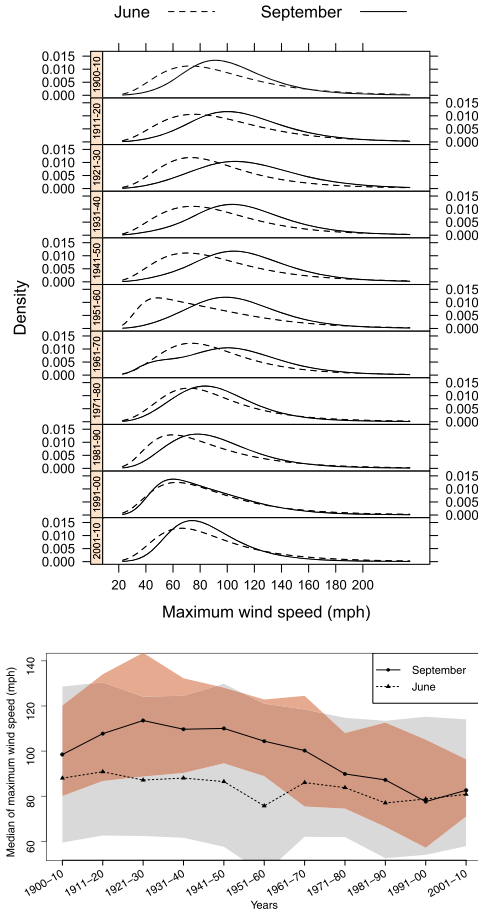
FIG. 8.   *Top panel*: *maximum wind speed densities conditional on June and September for all decades. Bottom panel*: *posterior expectation and* 95% *interval* (*dark gray band for September*; *light gray for June*) *for the median maximum wind speed in June and September versus decade.*

median standardized damage in the original scale. From 1900 to 1940, the estimated median standardized damage of one hurricane in ASO is around twice as large as that in MJJ. However, from 1941 to 2010, the median standardized damage in ASO depicts significant variability, with some indication of a slight decreasing trend across decades. These results are similar to the ones reported in Katz (2002) and Pielke et al. (2008), based on essentially the same data set, albeit under different damage normalization methods. In particular, Katz (2002) normalizes the damage during 1925–1995 to 1995 values and uses a log-normal distribution to fit the damage of individual storms, finding only weak evidence of a trend in the median of log-transformed damage. Likewise, in Pielke et al. (2008) hurricane damage is normalized to 2005 values. In this case, the conclusion is that there is no long-term increasing trend in hurricane damage during the 20th century, once
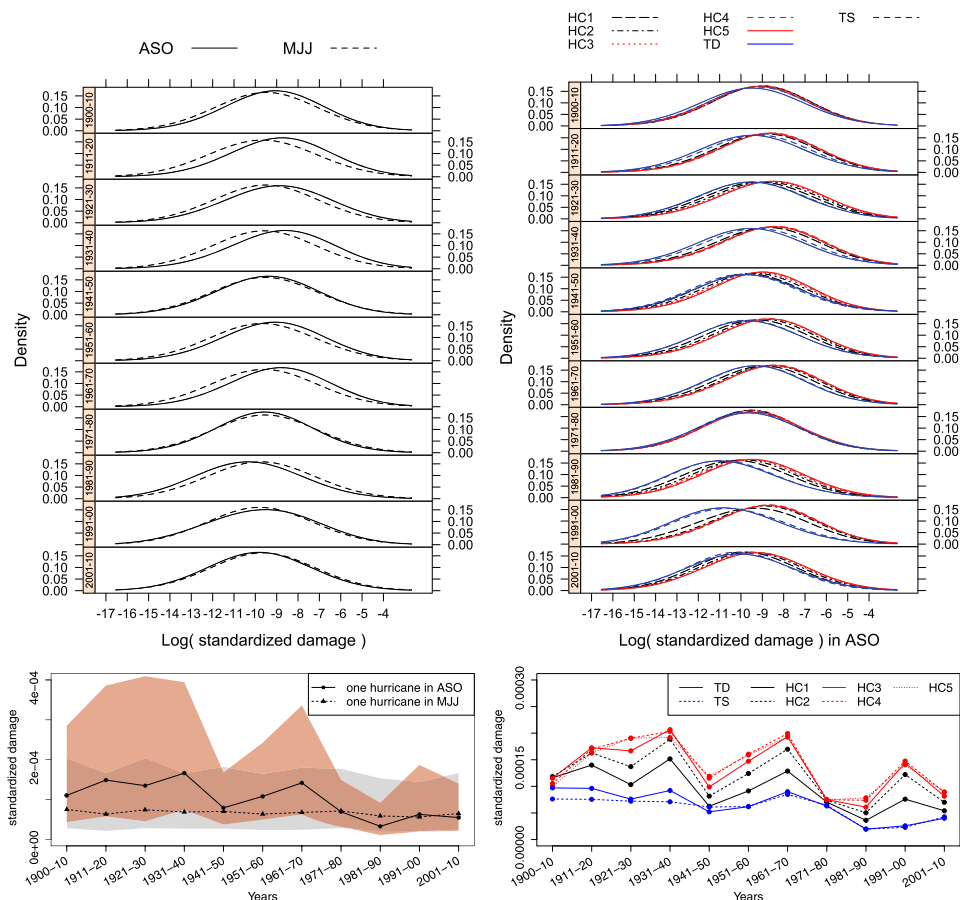
FIG. 9. *Top left panel*: *the density of logarithmic standardized damage conditional on MJJ* (*May–June–July*) *and ASO* (*August–September–October*). *Top right panel*: *the density of logarithmic standardized damage in ASO given the seven maximum wind speed categories defined in Table* 1. *Bottom left panel*: *Posterior expectation and* 95% *interval* (*dark gray band for ASO*; *light gray band for MJJ*) *for the median standardized damage of one hurricane in MJJ and ASO. Bottom right panel*: *Posterior expectation for the median standardized damage in ASO for the seven maximum wind speed categories.*

societal factors are removed. We also note here that Neumayer and Barthel (2011) detected a significant negative trend in hurricane damage. Their results are based on the same damage standardization method as the one we use, but for a different data set comprising hurricane damages from 1980–2009 in the U.S. and Canada.

The right-hand side panels of Figure 9 focus on the analysis of damage, conditional on the seven different types of hurricanes that occurred during ASO. The top panel reports the densities for logarithmic standardized damage conditional on the different hurricane categories. The bottom right panel reports the posterior expec-

tations for the corresponding median standardized damage. Overall, we observe that the higher the category, the larger the standardized damages tend to be. Standardized damages were very similar for the hurricanes recorded in ASO of decade 1971–1980, which is reflected in both types of inference shown in Figure 9. Standardized damages for TDs and TSs have indistinguishable distributions. Likewise, at the opposite end of the scale, damages due to HC4 and HC5 hurricanes are very similar. This is also due to the data sparseness of TDs and HC5 hurricanes (only 4 TDs and 3 HC5 hurricanes).

Figure 10 presents the bivariate densities of maximum wind speed and logarithmic standardized damage given the ASO period, for each decade. The last panel corresponds to the forecast density for 2011–2020. We note that only a handful of observations correspond to ASO in each particular decade. Thus, the results in Figure 10 are possible owing to our model's ability to borrow strength from all the available data. Noteworthy are the positive association between maximum wind speed and damage after the third decade, and the changes in the density shapes across the decades, especially 1961–1970 and 1991–2000. We also note the decrease in maximum wind speeds, starting in 1961–1970. Overall, from 1961, both the maximum wind speed and standardized damage have a general decreasing trend. This is a reflection of the fact that fewer hurricanes with extremely high maximum wind speed have occurred in recent decades. Regarding previous related work, Murnane and Elsner (2012) modeled the relationship between wind speed and normalized economic loss as exponential through quantile regression methods, using all hurricanes in the 20th century. Our methodology allows for a more comprehensive investigation of the relationship between hurricane damage and maximum wind speed, in particular, it enables study of its dynamic evolution across decades, without the need to rely on specific parametric regression forms.

4.5. *Model assessment.* The modeling approach is based on the assumption of a NHPP over the joint marks-points space. To check the NHPP assumption, we use the Time-Rescaling theorem [Daley and Vere-Jones (2003)], according to which, in each decade, the cumulative intensities between successive (ordered) observations, $\{\gamma_k \int_{t_{i-1,k}}^{t_{i,k}} f_k(t)\,dt\}$, are independent exponential random variables with mean one. Thus, $\{1 - \exp(-\gamma_k \int_{t_{i-1,k}}^{t_{i,k}} f_k(t)\,dt)\}$ are independent uniform$(0, 1)$ random variables. Likewise, the Poisson process assumption for the marks implies that the sets of random variables defined by the c.d.f. values of the conditional mark distributions, $\{F_k(y_{i,k}|t_{i,k})\}$ and $\{F_k(z_{i,k}|t_{i,k})\}$, are independent uniform$(0, 1)$ random variables. Hence, the NHPP assumption over both time and marks can be checked by using the MCMC output to obtain posterior samples for each of the three sets of random variables above, in each decade. Figure 11 shows the Q–Q plots of estimated quantiles for time, maximum wind speed and standardized damage versus the theoretical uniform distribution, for the last five decades. The results seem acceptable, especially in consideration of the limited sample sizes in each decade.
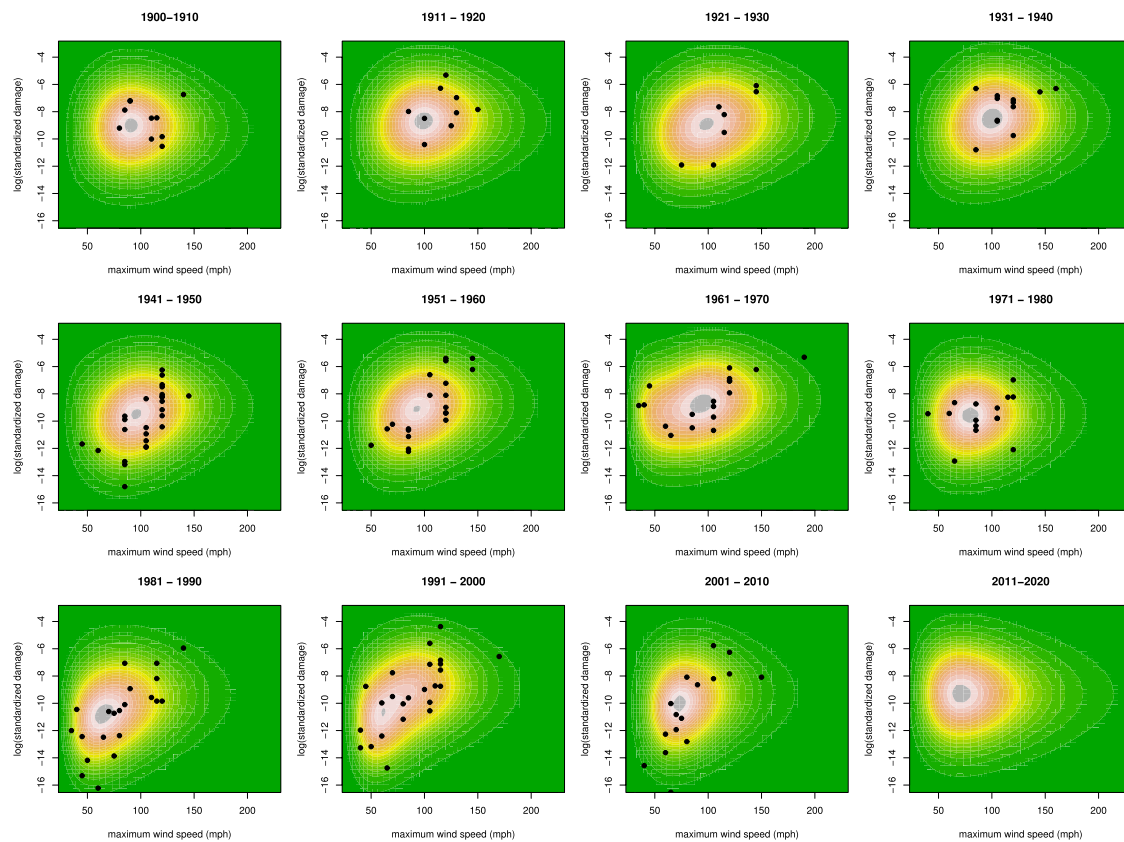
FIG. 10. *Bivariate densities of maximum wind speed* (*mph*) (*x-axis*) *and logarithmic standardized damage* (*y-axis*) *in ASO across decades. The dots correspond to observations in ASO.*
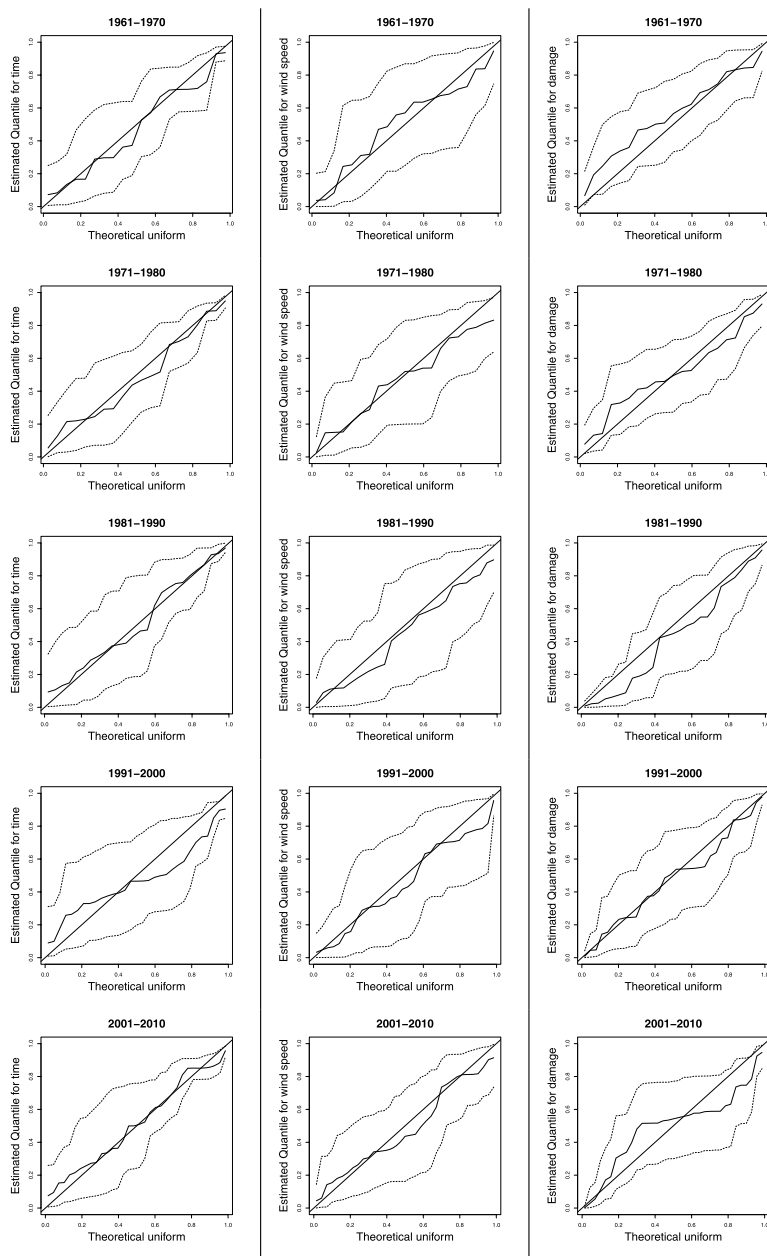
FIG. 11. *Posterior Q–Q plots* (*mean and* 95% *interval*) *of estimated quantiles against the the-oretical* uniform(0, 1) *for*: *time* (*left panel*), *maximum wind speed given time* (*middle panel*), *and standardized damage given time* (*right panel*). *Results are shown for the last five decades*.
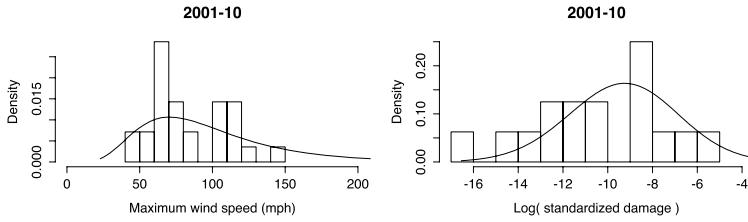
FIG. 12. *Cross-validated posterior predictive densities in ASO of decade* 2001–2010: *the left panel corresponds to maximum wind speed, and the right panel to logarithmic standardized damage. The histograms plot the associated observations in ASO of* 2001–2010.

As discussed earlier, Figures 5 and 6 provide visual goodness-of-fit evidence for the model on hurricane occurrences, by comparing different types of model-based inferences to the corresponding observations. Similar evidence is provided in Figure 10 for the maximum wind speed and log-damage relationship. We also explored other functionals of the model, obtaining similar results. In addition, we performed posterior predictive checks to study the model's ability to predict the marks in the 11th decade, based on the data of the previous 10 decades. In particular, we implemented the model using only the 204 hurricanes from 1900–2000, and obtained the posterior predictive density of maximum wind speed and logarithmic standardized damage in ASO of the 11th decade (2001–2010). Figure 12 shows the posterior predictive densities superimposed on the histograms of corresponding observations in ASO of 2001–2010. The histogram in the left panel corresponds to 28 hurricanes, whereas the one in the right panel corresponds to only 16 hurricanes, since the damages of the other 12 hurricanes are missing. We notice that the predictions are fairly compatible with the cross-validation data.

5. Conclusion. We have developed a Bayesian nonparametric modeling method for seasonal marked point processes and applied it to the analysis of hurricane landfalls with reported damages along the U.S. Gulf and Atlantic coasts from 1900 to 2010. Our basic assumption is that hurricane occurrences follow a nonhomogeneous Poisson process, with the focus on flexible modeling for dynamically evolving Poisson process intensities. The proposed DDP-PBAR model builds from a DDP mixture prior for the normalized intensity functions based on a PBAR process for the time-varying atoms, and a parametric time-varying model for the total intensities. Inference for different Poisson process functionals can be obtained by MCMC posterior simulation. To incorporate time-varying marks into the inferential framework for our motivating application, we have extended the DDP-PBAR mixture model by adding DDP-AR components for maximum wind speed and economic damages associated with each hurricane occurrence.

In the analysis of the hurricane data, we have used aggregation to study the dynamic evolution of hurricane intensity over decades. The model uncovers different shapes across decades which, however, share common features with respect to the off-season in May and June and the peak month of September. The results indicate an increase in the number of landfalling hurricanes and a decrease in the median maximum wind speed at the peak of the season across decades. In the off season, both the number of hurricanes and the maximum wind speed show little variation across decades. To study economic loss as a mark, we have introduced standardized damage to adjust hurricane damages such that they are comparable both in time and space. We found a slight decreasing trend in standardized damage of hurricanes in the peak season, which is also present conditional on the distinct hurricane categories.

With respect to the scientific context of the motivating application, our work provides a general framework to tackle different practically relevant problems. The key distinguishing feature of our approach relative to existing work involves the scope of the stochastic modeling framework under which the various inferences are obtained. As discussed in the Introduction, current work is limited to either estimating trends in hurricane occurrences at the annual level or estimating the hurricane intensity based on the fully aggregated data, thus ignoring dynamics across years. Moreover, when incorporating information on marks, existing approaches oversimplify the underlying point process structure by imposing homogeneity for the hurricane intensity. These assumptions are suspect, as demonstrated with the exploratory data analysis of Section 2. The proposed Bayesian nonparametric methodology enables flexible estimation of dynamically evolving, time-varying hurricane intensities within each season, and therefore has the capacity to capture trends during particular periods within the hurricane season. The full inferential power of the modeling framework is realized with the extension to incorporate marks, which are included as random variables in the joint model rather than as fixed covariates as in some of the previous work. From a practical point of view, the key feature of the model for the point process over the joint marks-points space is its ability to provide different types of general conditional inference, including full inference for dynamically evolving conditional mark densities given a time point, a particular time period and even a subset of marks.

In summary, the focus of this paper has been in developing a model that can quantify probabilistically the inter-seasonal and intra-seasonal variability of occurrence of a random process and its marks, jointly and without restrictive parametric assumptions. The model is particularly well suited for the description of irregular long-term trends, which may be present in the observations or in subsets of the records. To enhance the forecasting ability of the model, future work will consider extensions to incorporate external covariates (such as pre-season climate factors) in a similar fashion to Katz (2002), Jagger, Elsner and Burch (2011), and Elsner and Jagger (2013), albeit under the more general statistical modeling framework developed here.

APPENDIX: MCMC ALGORITHM FOR THE DDP-PBAR MODEL

The DDP-PBAR model for the data $\{t_{i,k}\}$ can be expressed as follows:

$$t_{i,k}|G_k, \tau \sim \int \text{Beta}(\mu\tau, (1-\mu)\tau) \, dG_k(\mu), \qquad i = 1, \dots, n_k; k = 1, \dots, K,$$

$$G_k(\mu) = \sum_{j=1}^{N} w_j \delta_{\mu_{j,k}}(\mu),$$

$$z_j \sim \text{Beta}(1, \alpha), \qquad w_1 = z_1;$$

$$w_j = z_j \prod_{r=1}^{j-1}(1 - z_r), \qquad j = 1, \dots, N-1;$$

$$w_N = 1 - \sum_{j=1}^{N-1} w_j,$$

$$\mu_{j,k} = v_{j,k} u_{j,k} \mu_{j,k-1} + (1 - v_{j,k}),$$

$$v_{j,k} \sim \text{Beta}(1, 1-\rho), \qquad u_{j,k} \sim \text{Beta}(\rho, 1-\rho).$$

We use an MCMC algorithm to draw posterior samples of $(\{\mu_{j,k}\}, \{v_{j,k}\}, \{w_j\}, \rho, \alpha)$, including blocked Gibbs sampling steps for the DDP prior parameters [Ishwaran and James (2001)]. Configuration variables $\{L_{i,k}\}$ are introduced to indicate the mixture component to which each observation is allocated. We use n^* to denote the number of distinct values in the $\{L_{i,k}\}$, and $L^* = \{L_j^* : j = 1, \dots, n^*\}$ for the set of distinct values.

The first step is to update the atoms $\{\mu_{j,k}\}$, which depends on whether j corresponds to an active component or not. When $j \notin L^*$, $\mu_{j,1} \sim \text{Unif}(0, 1)$, and for $k = 2, \dots, K$, $\mu_{j,k}$ is drawn from $p(\mu_{j,k}|\mu_{j,k-1}, v_{j,k}, \rho)$, which is a scaled Beta distribution arising from the PBAR process,

$$p(\mu_{j,k}|\mu_{j,k-1}, v_{j,k}, \rho) = \frac{1}{v_{j,k}\mu_{j,k-1}} \text{Beta}\left(\frac{\mu_{j,k} + v_{j,k} - 1}{v_{j,k}\mu_{j,k-1}} \Big| \rho, 1 - \rho\right),$$

where $\mu_{j,k} \in (1 - v_{j,k}, \min\{1, 1 - v_{j,k} + v_{j,k}\mu_{j,k-1}\})$. When $j \in L^*$, the posterior full conditional for $\mu_{j,1}$ is proportional to $\prod_{i=1,\{L_{i,1}=j\}}^{N_1} \text{Beta}(t_{i,1}|\mu_{j,1}\tau, (1 - \mu_{j,1})\tau) p(\mu_{j,2}|\mu_{j,1}, v_{j,2}, \rho) p(\mu_{j,1})$. For $k = 2, \dots, K - 1$, the full conditional for $\mu_{j,k}$ is proportional to $\prod_{i=1,\{L_{i,k}=j\}}^{N_k} \text{Beta}(t_{i,k}|\mu_{j,k}\tau, (1 - \mu_{j,k})\tau) p(\mu_{j,k+1}|\mu_{j,k}, v_{j,k+1}, \rho) p(\mu_{j,k}|\mu_{j,k-1}, v_{j,k}, \rho)$. Finally, the full conditional for $\mu_{j,K}$ is proportional to $\prod_{i=1,\{L_{i,K}=j\}}^{N_K} \text{Beta}(t_{i,K}|\mu_{j,K}\tau, (1 - \mu_{j,K})\tau) p(\mu_{j,K}|\mu_{j,K-1}, v_{j,K}, \rho)$. We use Metropolis–Hastings steps to update the $\mu_{j,k}$, with the proposal distribution taken to be $p(\mu_{j,k}|\mu_{j,k-1}, v_{j,k}, \rho)$.

The sampling of weights $\{w_j\}$, configuration variables $\{L_{i,k}\}$ and α can be implemented using standard updates under the blocked Gibbs sampler. Updating the

latent variables $\{v_{j,k}\}$ involves only the PBAR process. The full conditionals are given by

$$
p(v_{j,k}|\mu_{j,k}, \mu_{j,k-1}, \rho)
$$
$$
\propto \frac{1}{v_{j,k}} \operatorname{Beta}\left(\frac{\mu_{j,k} + v_{j,k} - 1}{v_{j,k}\mu_{j,k-1}} \Big| \rho, 1 - \rho\right) \operatorname{Beta}(v_{j,k}|1, 1 - \rho),
$$

where $v_{j,k} \in (1 - \mu_{j,k}, \min\{1, \frac{1-\mu_{j,k}}{1-\mu_{j,k-1}}\})$, and sampling from each of them was implemented with a Metropolis–Hastings step based on $\operatorname{Beta}(1, 1 - \rho)$ as the proposal distribution. Finally, the PBAR correlation parameter ρ is also sampled using a Metropolis–Hastings step.

REFERENCES

ADAMS, R. P., MURRAY, I. and MACKAY, D. J. C. (2009). Tractable nonparametric Bayesian inference in Poisson processes with Gaussian process intensities. In *Proceedings of the 26th International Conference on Machine Learning*, Montreal, Canada.

ANTONIAK, C. E. (1974). Mixtures of Dirichlet processes with applications to Bayesian nonparametric problems. *Ann. Statist.* **2** 1152–1174. MR0365969

BRIX, A. and DIGGLE, P. J. (2001). Spatiotemporal prediction for log-Gaussian Cox processes. *J. R. Stat. Soc. Ser. B. Stat. Methodol.* **63** 823–841. MR1872069

CHAVAS, D. R., YONEKURA, E., KARAMPERIDOU, C., CAVANAUGH, N. and SERAFIN, K. (2012). U.S. Hurricanes and economic damage: An extreme value perspective. *Natural Hazards Review* **14** 237–246.

COLLINS, D. J. and LOWE, S. P. (2001). A macro validation dataset for U.S. hurricane models. In *Casualty Actuarial Society Forum* 217–252. Casualty Actuarial Society, Arlington, VA.

DALEY, D. J. and VERE-JONES, D. (2003). *An Introduction to the Theory of Point Processes. Vol. I*: *Elementary Theory and Methods*, 2nd ed. Springer, New York. MR1950431

ELSNER, J. B. and JAGGER, T. H. (2013). *Hurricane Climatology*: *A Modern Statistical Guide Using R*. Oxford Univ. Press, Oxford. MR3051752

ELSNER, J. B., XU, F. N. and JAGGER, T. H. (2004). Detecting shifts in hurricane rates using a Markov chain Monte Carlo approach. *Journal of Climate* **17** 2652–2666.

EMANUEL, K. (2005). Increasing destructiveness of tropical cyclones over the past 30 years. *Nature* **436** 686–688.

FERGUSON, T. S. (1973). A Bayesian analysis of some nonparametric problems. *Ann. Statist.* **1** 209–230. MR0350949

GAMERMAN, D., REZENDE DOS SANTOS, T. and FRANCO, G. C. (2013). A non-Gaussian family of state–space models with exact marginal likelihood. *J. Time Series Anal.* **34** 625–645. MR3127211

IHLER, A. T. and SMYTH, P. J. (2007). Learning time-intensity profiles of human activity using non-parametric Bayesian models. In *Neural Information Processing Systems* 19 (B. Schölkopf, J. Platt and T. Hoffman, eds.) 625–632. MIT Press, Cambridge, MA.

ISHWARAN, H. and JAMES, L. F. (2001). Gibbs sampling methods for stick-breaking priors. *J. Amer. Statist. Assoc.* **96** 161–173. MR1952729

ISHWARAN, H. and JAMES, L. F. (2004). Computational methods for multiplicative intensity models using weighted gamma processes: Proportional hazards, marked point processes, and panel count data. *J. Amer. Statist. Assoc.* **99** 175–190. MR2054297

JAGGER, T. H. and ELSNER, J. B. (2006). Climatology models for extreme hurricane winds near the United States. *Journal of Climate* **19** 3220–3236.

JAGGER, T., ELSNER, J. and BURCH, R. (2011). Climate and solar signals in property damage losses from hurricanes affecting the United States. *Natural Hazards* **58** 541–557.

JI, C., MERL, D., KEPLER, T. B. and WEST, M. (2009). Spatial mixture modelling for unobserved point processes: Examples in immunofluorescence histology. *Bayesian Anal.* **4** 297–315. MR2507365

KATZ, R. W. (2002). Stochastic modeling of hurricane damage. *Journal of Applied Meteorology* **41** 754–762.

KATZ, R. W. (2010). Statistics of extremes in climate change. *Climatic Change* **100** 71–76.

KOTTAS, A. (2006). Dirichlet process mixtures of Beta distributions, with applications to density and intensity estimation. In *Proceedings of the Workshop on Learning with Nonparametric Bayesian Methods*, 23rd *International Conference on Machine Learning*, Pittsburgh, PA.

KOTTAS, A. and SANSÓ, B. (2007). Bayesian mixture modeling for spatial Poisson process intensities, with applications to extreme value analysis. *J. Statist. Plann. Inference* **137** 3151–3163. MR2365118

KOTTAS, A., WANG, Z. and RODRÍGUEZ, A. (2012). Spatial modeling for risk assessment of extreme values from environmental time series: A Bayesian nonparametric approach. *Environmetrics* **23** 649–662. MR3019057

KOTTAS, A., BEHSETA, S., MOORMAN, D., POYNOR, V. and OLSON, C. (2012). Bayesian nonparametric analysis of neuronal intensity rates. *Journal of Neuroscience Methods* **203** 241–253.

LANDSEA, C. W. (1993). A climatology of intense (or major) Atlantic hurricanes. *Monthly Weather Review* **121** 1703–1713.

LANDSEA, C., PIELKE, R. A., MESTAS-NUÑEZ, A. and KNAFF, J. (1999). Atlantic Basin hurricanes: Indices of climatic changes. *Climatic Change* **42** 89–129.

LIANG, S., CARLIN, B. P. and GELFAND, A. E. (2009). Analysis of Minnesota colon and rectum cancer point patterns with spatial and nonspatial covariate information. *Ann. Appl. Stat.* **3** 943–962. MR2750381

MACEACHERN, S. N. (1999). *Dependent Nonparametric Processes*. American Statistical Association, Alexandria, VA.

MACEACHERN, S. N. (2000). Dependent Dirichlet processes. Technical report, Dept. Statistics, Ohio State Univ.

MCKENZIE, E. (1985). An autoregressive process for Beta random variables. *Management Science* **31** 988–997.

MØLLER, J., SYVERSVEEN, A. R. and WAAGEPETERSEN, R. P. (1998). Log Gaussian Cox processes. *Scand. J. Stat.* **25** 451–482. MR1650019

MØLLER, J. and WAAGEPETERSEN, R. P. (2004). *Statistical Inference and Simulation for Spatial Point Processes*. *Monographs on Statistics and Applied Probability* **100**. Chapman & Hall/CRC, Boca Raton, FL. MR2004226

MURNANE, R. J. and ELSNER, J. B. (2012). Maximum wind speeds and US hurricane losses. *Geophysical Research Letters* **39** L16707.

NEUMAYER, E. and BARTHEL, F. (2011). Normalizing economic loss from natural disasters: A global analysis. *Global Environmental Change* **21** 13–24.

PARISI, F. and LUND, R. (2000). Seasonality and return periods of landfalling Atlantic Basin hurricanes. *Aust. N. Z. J. Stat.* **42** 271–282.

PIELKE, R. A. JR. and PIELKE, R. A. (1997). *Hurricanes*: *Their Nature and Impacts on Society*. Wiley, London.

PIELKE, R. A. JR., GRATZ, J., LANDSEA, C. W., COLLINS, D., SAUNDERS, M. A. and MUSULIN, R. (2008). Normalized hurricane damage in the United States: 1900–2005. *Natural Hazards Review* **9** 29–42.

ROBBINS, M. W., LUND, R. B., GALLAGHER, C. M. and LU, Q. (2011). Changepoints in the North Atlantic tropical cyclone record. *J. Amer. Statist. Assoc.* **106** 89–99. MR2816704

SCHMIDT, S., KEMFERT, C. and HOEPPE, P. (2010). The impact of socio-economics and climate change on tropical cyclone losses in the USA. *Regional Environmental Change* **10** 13–26.

SETHURAMAN, J. (1994). A constructive definition of Dirichlet priors. *Statist. Sinica* **4** 639–650. MR1309433

SOLOW, A. R. (1989). Statistical modeling of storm counts. *Journal of Climate* **2** 131–136.

TADDY, M. A. (2010). Autoregressive mixture models for dynamic spatial Poisson processes: Application to tracking intensity of violent crime. *J. Amer. Statist. Assoc.* **105** 1403–1417. MR2796559

TADDY, M. A. and KOTTAS, A. (2012). Mixture modeling for marked Poisson processes. *Bayesian Anal.* **7** 335–361. MR2934954

WOLPERT, R. L. and ICKSTADT, K. (1998). Poisson/gamma random field models for spatial statistics. *Biometrika* **85** 251–267. MR1649114

DEPARTMENT OF APPLIED MATHEMATICS AND STATISTICS
UNIVERSITY OF CALIFORNIA, SANTA CRUZ
SANTA CRUZ, CALIFORNIA 95064
USA
E-MAIL: sxiao@soe.ucsc.edu
         thanos@soe.ucsc.edu
         bruno@soe.ucsc.edu